Experimental Research

INTERNATIONAL JOURNAL OF SURGERY

OPEN

Tibial cortex transverse transport surgery improves wound healing in patients with severe type 2 DFUs by activating a systemic immune response: a cross-sectional study

Lin Yu, PhD[a,b,*], Dingwei Zhang, MSc[c], Yuan Yin, PhD[b], Xiaoya Li, MBBS[c], Chunxia Bai, MBBS[c], Qian Zhou, BSc[a], Xinyi Liu, BSc[a], Xiaojun Tian, MBBS[a], Daofei Xu, MSc[c], Xianjun Yu, MBBS[c], Sichun Zhao, MSc[c], Rong Hu, MSc[c], Fudie Guo, MBBS[c], Yuwei Yang, MBBS[a], Yan Ren, MSc[a], Gang Chen, MBBS[a], Jiawei Zeng, PhD[a], Jiafu Feng, PhD[a]

Background: Tibial cortex transverse transport (TTT) surgery has become an ideal treatment for patients with type 2 severe diabetic foot ulcerations (DFUs), while conventional treatments are ineffective. Based on our clinical practice experience, the protective immune response from TTT surgery may play a role against infections to promote wound healing in patients with DFUs. Therefore, this research aimed to systematically study the specific clinical efficacy and the mechanism of TTT surgery.

Materials and methods: Between June 2022 and September 2023, 68 patients with type 2 severe DFUs were enrolled and therapized by TTT surgery in this cross-sectional and experimental study. Major clinical outcomes, including limb salvage rate and antibiotics usage rate, were investigated. Ten clinical characteristics and laboratory features of glucose metabolism and kidney function were statistically analyzed. Blood samples from six key time points of TTT surgery were collected for label-free proteomics and clinical immune biomarker analysis. Besides, tissue samples from three key time points were used for spatially resolved metabolomics and transcriptomics analysis, as well as applied to validate the key TTT-regulated molecules by reverse-transcription quantitative PCR.

Results: Notably, 64.7% of patients did not use antibiotics during the entire TTT surgery. TTT surgery can achieve a high limb salvage rate of 92.6% in patients with unilateral or bilateral DFUs. Pathway analysis of a total of 252 differentially expressed proteins from the proteomic revealed that the immune response induced by TTT surgery at different stages was first comprehensively verified through multiomics combined with immune biomarker analysis. The function of upward transport was activating the systemic immune response, and wound healing occurs with downward transport. The spatial metabolic characteristics of skin tissue from patients with DFUs indicated downregulated levels of stearoylcarnitine and the glycerophospholipid metabolism pathway in skin tissue from patients with severe DFUs. Finally, the expressions of PRNP (prion protein) to activate the immune response, PLCB3 (phospholipase C beta 3) and VE-cadherin play roles in neovascularization, and PPDPF (pancreatic progenitor cell differentiation and proliferation factor), LAMC2 (laminin subunit gamma 2), and SPRR2G (small proline-rich protein 2G) to facilitate the developmental process mainly keratinocyte differentiation were statistically significant in skin tissues through transcriptomic and reverse-transcription quantitative PCR analysis.

Conclusion: TTT surgery demonstrates favorable outcomes for patients with severe type 2 DFUs by activating a systemic immune response, contributing to anti-infection, ulcer recurrence, and the limb salvage for unilateral or bilateral DFUs. The specific clinical immune responses, candidate proteins, genes, and metabolic characteristics provide directions for in-depth mechanistic research on TTT surgery. Further research and public awareness are needed to optimize TTT surgery in patients with severe type 2 DFUs.

Keywords: diabetic foot ulceration, tibial cortex transverse transport surgery, wound healing, limb salvage rate, immune response, multi-omics, clinical immune biomarker

[a]Department of Clinical Laboratory, Mianyang Central Hospital, School of Medicine, University of Electronic Science and Technology of China, [b]NHC Key Laboratory of Nuclear Surgery Medical Transformation, Mianyang Central Hospital, School of Medicine, University of Electronic Science and Technology of China and [c]Department of Orthopaedics, Mianyang Central Hospital, School of Medicine, University of Electronic Science and Technology of China, Mianyang, China

L.Y., D.Z., Y.Y. contributed equally to this work.

Sponsorships or competing interests that may be relevant to content are disclosed at the end of this article.

**Corresponding author. Address. No.12, Changjia Lane, Fucheng District, Mianyang City, Sichuan Province 621000, China, Tel.: +816 220 2396. E-mail: linyu@sc-mch.cn (L. Yu).*

International Journal of Surgery (2025) 111:257–272

Received 1 March 2024; Accepted 18 June 2024

Supplemental Digital Content is available for this article. Direct URL citations are provided in the HTML and PDF versions of this article on the journal's website, www.lww.com/international-journal-of-surgery.

Published online 2 July 2024

http://dx.doi.org/10.1097/JS9.0000000000001897

Introduction

DFU is a serious complication of type 2 diabetes patients[1–3]. Unfortunately, 90% of DFU patients with Wagner grade III or above eventually require amputation, and the 5-year mortality rate after amputation is as high as 25–50%[4–6]. Therefore, it is of important clinical significance to explore new treatments to improve the outcome and reduce the amputation rate for patients with type 2 severe DFUs. Derived from the theory of the Ilizarov technique, TTT surgery has become an ideal treatment for patients with DFUs when conventional treatments are ineffective in clinical practice[7–9]. However, there is a lack of systematic research on the efficacy as well as the molecular mechanism of TTT surgery.

To study the efficacy of the TTT surgery, 68 patients with type 2 severe DFUs receiving TTT surgery were enrolled. Major clinical outcomes (limb salvage rate and antibiotics usage rate) and secondary indicators (laboratory features of glucose metabolism and kidney function) were statistically investigated. To date, our team has effectively applied TTT surgery to treat more than 1000 patients with type 2 severe DFUs, achieving a favorable limb salvage rate, the same for those who were without the use of antibiotics during the entire treatment process. More importantly, ideal effects can be observed in patients with bilateral DFUs, even when TTT surgery is carried out on only one side with a higher Wagner score. Based on our clinical practice, we speculate that the immune system plays an important role. However, the specific immune changes associated with the anti-infection effect of TTT surgery on promoting wound healing are still unclear.

Recent growth in the field of immunometabolism has revealed how specific changes in the concentrations of metabolites in immune cells can affect the immune response. The consequences of these metabolic alterations go beyond the traditional role of metabolism in bioenergetics and biosynthesis[10]. The interaction of proteins is emerging as a key means by which intracellular metabolites can modulate immunity[11,12]. To date, proteomics, transcriptomics, and spatial metabolomics studies have fundamentally improved our understanding of immunobiology and optimized clinical therapeutic strategies for disease[13–15]. Immunomodulatory proteins at different stages can be authenticated by proteomics analysis. Mass spectrometry imaging-based spatially resolved metabolomics allows in situ screening of immune-related metabolic biomarkers, thus allowing for the characterization of the metabolic architecture of disease and its surrounding microenvironment. Transcriptomics technologies provide a broad account of which immune response and wood healing are active and which are dormant[16]. Through integrated analysis of multiomics data, we can comprehensively and systematically understand the key factors involved in the occurrence and development of diseases. Understanding the interrelationship between substances provides important technical means for the study of the immunological biology of diseases[13]. Here, we propose an integrated multiomics approach to provide direct evidence that TTT surgery activates a systemic immune response to effectively treat unilateral or bilateral DFUs in patients with severe type 2 DFUs.

HIGHLIGHTS

- TTT surgery can treat type 2 severe diabetic foot ulcerations (DFUs) patients with good clinical outcomes.
- Upward transport started to activate the systemic immune response.
- Wound healing initially occurs during the downward transport stage.
- Stearoylcarnitine and the glycerophospholipid metabolism pathway were downregulated.
- Candidate genes regulated by TTT surgery to activate the immune response and promote wound healing were validated.

Research design and methods

Study population

Patients with type 2 severe DFUs were consecutively recruited from June 2022 to September 2023 and underwent TTT surgery according to the clinical criteria. A total of 68 patients were included: 63 patients had unilateral DFUs, and 5 patients had bilateral DFUs. The inclusion criteria were as follows: patients with DFUs in Wagner grade III or above[17] and patients with partial arterial recanalization below the popliteal artery as detected by ultrasound Doppler, computed tomography angiography, magnetic resonance angiography, or digital subtraction angiography. The prerequisites for vascular reconstruction were that the superficial femoral artery and popliteal artery were unobstructed and that at least one of the anterior tibial arteries, posterior tibial artery, or peroneal arteries were unobstructed to the ankle joint plane. Most importantly, the patients agreed to undergo TTT surgery. The exclusion criteria were as follows: patients with mental illness; patients diagnosed by an endocrinologist with other severe complications of diabetes, such as systemic infection or uncontrolled deep infection; patients with cardiovascular complications or renal failure; patients with anesthesia intolerance; patients with obstruction of the superficial femoral artery or popliteal artery; or patients without any arterial branch (anterior tibial, posterior tibial, or peroneal artery) blood supply to the calf. Our work has been reported in line with the STROCSS criteria[18].

Tibial cortex transverse transport surgery protocol and biospecimens

The TTT surgical procedure is described in detail in Figure 1 and Figure 2A. To ensure quality, all surgeries were done by a regular skilled surgical and nursing team. Before TTT surgery, TTT external fixators (two long screws, two small screws, a turning nut, and an external fixator frame) were prepared. Next, two small longitudinal incisions (1 cm) in the ready tibia were exposed and guided with an external fixator, and the installation steps were performed according to standard operating procedures. Finally, a silicone splint was fixed to the wound leg[19]. Whether patients suffered from unilateral or bilateral DFUs, TTT surgery was applied on only one side with a higher Wagner score. The most important procedures of TTT surgery were upward transport (7 mm, 1 mm/day) and downward transport (7 mm, 1 mm/day) for one cycle, with a total of 14 days. In total, the workflows and time points of TTT technology procedures were as follows: 1 day before the TTT external fixator was fixed (TTT_0), 3 days after the TTT external fixator was fixed (TTT_3), 7 days after the TTT external fixator was fixed (TTT_7), the day which the upward transport was completed (TTT_{14}), the day which the downward

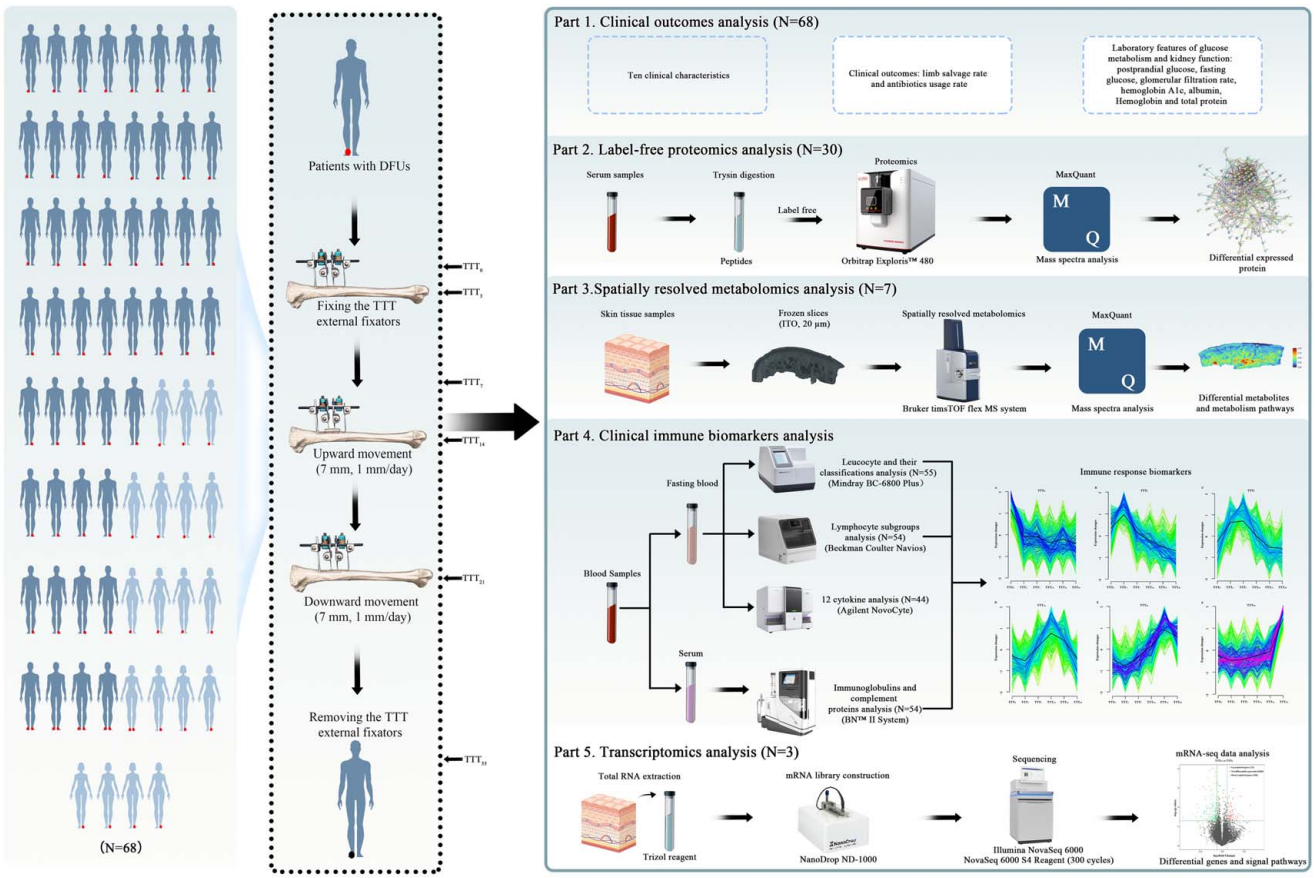

Figure 1. The design and workflow of this study. This study mainly contained four parts. First, 68 patients with unilateral or bilateral DFUs were treated with TTT surgery, and samples at six key time points were collected for the study. Second, label-free proteomic analysis of immunomodulatory proteins and regulatory pathways ($N = 30$, TTT_0, TTT_3, TTT_7, TTT_{14}, TTT_{21}, and TTT_{35}) was performed. Third, skin tissue samples from three key time points were collected for spatial metabolomics to validate the immunological metabolites ($N = 7$, TTT_0, TTT_{14}, and TTT_{21}). Next, the specific immune biomarkers were validated in the clinical laboratory (TTT_0, TTT_3, TTT_7, TTT_{14}, TTT_{21}, and TTT_{35}). In addition, transcriptomics analysis for skin tissue samples was applied to screen out differential genes and signal pathways in regulating the immune response and wound healing ($N = 3$, TTT_0, TTT_{14}, and TTT_{21}). Finally, the integration of data from multiomic and clinical immune biomarker analyses was applied to investigate possible immune responses. N, the number of patients; TTT_0, 1 day before the TTT external fixator was fixed; TTT_3, 3 days after the TTT external fixator was fixed; TTT_7, 7 days after the TTT external fixator was fixed; TTT_{14}, the day at which the upward movement was completed; TTT_{21}, the day at which the downward transfer was completed; TTT_{35}, the second day after the TTT external fixator was removed. DFU, diabetic foot ulceration; TTT, tibial cortex transverse transport.

transfer was completed (TTT_{21}), and the second day after the TTT external fixator was removed (TTT_{35}). At the above-mentioned time points, the skin tissues were subjected to spatially resolved metabolomics ($N = 7$, TTT_0, TTT_{14}, and TTT_{21}) and transcriptomics ($N = 3$, TTT_0, TTT_{14}, and TTT_{21}) analysis, the serum samples ($N = 30$, TTT_0, TTT_3, TTT_7, TTT_{14}, TTT_{21}, and TTT_{35}) were subjected to label-free proteomics analysis, and fasting blood samples (TTT_0, TTT_3, TTT_7, TTT_{14}, TTT_{21}, and TTT_{35}) were collected for the remaining study. All fasting blood samples were collected after routine examinations.

Clinical outcomes analysis

Clinical characteristics were collected, including gender, age, diabetes history, time for wound healing, diabetic eye disease, cardiovascular disease, glycemic control effect, location of DFUs, Wagner classification, and diabetic kidney disease. Major clinical outcomes of patients after postoperative, including limb salvage rate and antibiotics usage rate, were statistically investigated. Thirteen clinical characteristics and laboratory features of glucose metabolism and kidney function were statistically analyzed. Albumin (g/l), postprandial glucose (mmol/l), fasting glucose (mmol/l), the glomerular filtration rate (ml/min), and total protein (g/l) were measured with a LABOSPECT 008 α (Hitachi High-Tech Corporation, Japan). Hemoglobin A1c (%) and hemoglobin (g/l) were measured with an MQ-6000 (Shanghai Huizhong Corporation, China). The ankle–brachial index and other clinical parameters were measured and recorded by a nurse and clinician according to standard operating procedures. Age, diabetes history, and time to wound healing were analyzed by the independent sample t test, and a continuous corrected four-grid table or contingency table χ^2 test was used for the remaining parameters. As described above, the collection, description, and comparison of information on TTT surgery on patients with DFUs at a specific point in time, thus providing clues to TTT surgery for further research. So, this study is a cross-sectional and experimental study.

Label-free proteomics analysis

First, 30 patients with 180 samples (TTT_0, TTT_3, TTT_7, TTT_{14}, TTT_{21}, and TTT_{35}) were prepared for label-free proteomics

Figure 2. TTT surgical procedure and significant therapeutic effects on patients with type 2 severe DFUs. (A) Process diagram of TTT surgery in patients with unilateral or bilateral DFUs. For unilateral or bilateral DFUs, TTT surgery was only applied on one side with a higher Wagner score. The key management methods used for TTT were upward transport (7 mm, 1 mm/day) and downward transport (7 mm, 1 mm/day) for one cycle for a total of 14 days. When patients suffered from unilateral or bilateral DFUs, TTT surgery was applied on only one side with a high Wagner score. Typical clinical case of TTT surgery effectively treating patients with unilateral (B and C) or bilateral (D) DFUs. DFU, diabetic foot ulceration; TTT, tibial cortex transverse transport.

analysis. To reduce errors associated with individual differences, serum samples from each of the six patients at the same time point were mixed into one sample. Finally, 30 mixed samples were analyzed, and the details of the proteomics analysis have also been described previously. First, magnetic separation was used to obtain intact protein samples, and enzymatic desalination was used to obtain peptide fragments for mass spectrometry (MS) detection. Afterwards, the Orbitrap Exploris 480 MS system was applied for MS detection in all samples, and Xcalibur software (Thermo, USA) was used for data collection. Finally, bioinformatics analysis (peptide and protein qualitative analysis, superiority comparison of new methods, differential protein quantitative analysis, GO analysis, and pathway analysis) was used for most analyses. For the label-free proteomics analysis in our study, the differentially expressed proteins (DEPs) were identified by *t* tests with fold change (FC) values ≥ 1.2 or FC $\leq$ 0.3 and *P* values < 0.05 for comparisons between two time points. Gene ontology (GO) enrichment from cellular components, molecular function, and biological process and Kyoto Encyclopedia of Genes and Genomes (KEGG) pathway enrichment analyses were performed by Fisher's exact test, considering the whole quantified protein annotations as the background dataset. The *P* values obtained from enrichment analysis were further converted into *q* values using Benjamini–Hochberg correction, and a *q* value less than 0.05 was considered significant[20,21].

Spatially resolved metabolomics analysis

Frozen tissue samples were fixed in three drops of distilled water during the cutting stage. The tissues were sectioned at a thickness of 10 μm using a Leica CM1950 cryostat (Leica Microsystems GmbH, Wetzlar, Germany) at −20°C. Afterward, the tissue sections were placed in groups on electrically conductive slides coated with indium tin oxide, and the brain sections were dried in a vacuum desiccator for 30 min. Matrix-assisted laser desorption/ionization timsTOF MSI experiments were performed on a prototype Bruker timsTOF flex MS system (Bruker Daltonics, Bremen, Germany) equipped with a 10 kHz smartbeam 3D laser. The laser power was set to 70%, and the samples were then fixed throughout the entire experiment. The mass spectra were acquired in negative mode. The mass spectra data were acquired over a mass range from *m/z* 50–1300 Da. The imaging spatial resolution was set to 100 μm for the tissue, and each spectrum consisted of 400 laser shots. The matrix-assisted laser desorption/ionization mass spectra were normalized to the root mean square, and the signal intensity in each image is shown as the normalized intensity. MS/MS fragmentations performed on the timsTOF flex MS system in MS/MS mode were used for further detailed structural confirmation of the identified metabolites. The in-depth bioinformatic analysis procedure was performed according to published studies[22].

Clinical immune biomarkers analysis

Fasting blood and serum samples were obtained from patients with DFUs at six-time points in the morning. Due to amputation, death, and unable to test in time for holidays, the number of patients enrolled in clinical immune biomarker analysis was not the same. First, the clinical immune biomarkers included leukocytes and their subtypes (lymphocytes, monocytes, neutrophils, eosinophils, and basophils), lymphocyte subgroups ($CD3^+$ lymphocytes %, $CD3^+CD4^+$ lymphocytes %, $CD3^+CD8^+$ lymphocytes %, $CD4^+/CD8^+$ ratio, $CD19^+$ lymphocytes %, $CD16^+$ $CD56^+$ NK cells %, $CD45^+$ lymphocyte AVs, $CD3^+$ lymphocyte AVs, $CD19^+$ lymphocyte AVs, $CD16^+CD56^+$ NK cell AVs, $CD3^+CD4^+$ lymphocyte AVs), 12 cytokines (IL-2, IL-6, IL-10, IFN-γ, TNFα, IL-4, IL-1β, IL-5, IL-12P70, IL-17, IFN-α, and IL-8), humoral immunity makers (IgG, IgA, IgM, IgE, κ and λ), and complement proteins (C3 and C4).

Then, whole blood samples were prepared for leukocyte and classification analysis (Mindray BC-6800 Plus; Mindray Corporation, China) and lymphocyte subset analysis (Beckman Coulter Navios; Beckman Coulter Inc., USA), while serum samples were used for 12 cytokine analyses (Agilent NovoCyte; Agilent Technologies Inc., USA) and immunoglobulin and complement protein analyses (BN II System; Siemens Healthcare Diagnostics Products GmbH, Germany).

Total RNA extraction

Human skin tissues at TTT_0, TTT_{14}, and TTT_{21} from patients with type 2 severe DFUs were chosen for RNA extraction. Every 50 mg of tissue sample was added into 1 ml of Trizol reagent and homogenized using an electric homogenizer. Then, total RNA was extracted from the tissues using Trizol (Invitrogen, Carlsbad, CA, USA) according to manual instructions. Subsequently, total RNA was qualified and quantified using NanoDrop ND-1000 to determine RNA concentration and purity and denaturing agarose gel electrophoresis to exclude DNA contamination and RNA degradation.

mRNA library construction

Total RNA was extracted using TRIzol Reagent (Invitrogen), and RNA concentration was determined using NanoDrop ND-1000. After removing the rRNAs, 2 μg of total RNA was used for the preparation of the cDNA library with a KAPA-Stranded RNA-Seq Library Prep Kit (Illumina, USA). The total RNA was processed by NEBNext Poly(A) mRNA Magnetic Isolation Module (or rRNA removal by RiboZero Magnetic Gold Kit) to enrich mRNA, and the product RNA was used for construction library via KAPA-Stranded RNA-Seq Library Prep Kit (Illumina). The constructed libraries were subjected to quality control (library concentration, fragment size 400–600 bp, and presence or absence of junctions) by Agilent 2100 Bioanalyzer, and the final quantification of the libraries was performed by quantitative PCR. According to the quantitative results and the final sequencing data volume requirements, the sequencing libraries of different samples were mixed into the sequencing process. Mixed sequencing libraries of different samples were denatured into single-stranded DNA by 0.1 M NaOH, diluted to a concentration of 8 pM, and amplified in situ via NovaSeq 6000 S4 Reagent (300 cycles). Finally, the ends of the fragments were sequenced for 150 cycles using Illumina NovaSeq 600[23,24].

mRNA-seq data analysis

The quantitative analysis of gene expression was performed at Gene Level and Transcript Level, which was obtained by the software StringTie by comparing the results to known transcriptomes, performing transcript abundance calculations, and then by Ballgown calculations, and the unit of expression was expressed as FPKM (Fragments Per Kilobase of gene/transcript

model per million mapped fragments). The genes or transcripts with an average FPKM of more than 0.5 in each group are regarded as being expressed in the subgroups. Then, the quantitative analyses of the expression of the gene and transcript, analyses based on the level of gene expression, screening for differentially expressed genes, and other analyses, such as quantitative gene and transcript expression analysis, gene expression level-based analysis, differential gene expression screening, GO functional significance enrichment analysis, pathway significance enrichment analysis, and so on. Finally, we have drawn scatter plots, volcano plots, cluster plots, and other rich visualization views to facilitate the browsing of the data.

Reverse-transcription quantitative PCR

RNA samples were prepared as described as part of total RNA extraction. Equal quantities (5 ng) of total RNA from each sample were used for cDNA synthesis using the All-In-One 5×RT Mastermix cDNA Synthesis Kit (Abcam, #G592). The reverse transcriptions of validated genes were performed by looped miRNA-specific RT primers (Supplementary Table S5) for miRNAs. Reverse-transcription quantitative (RT-qPCR) was performed using BlastaqTM 2×qPCR Mastermix (Abcam, #G891) for the detection of mRNA expression level. The internal control was β-actin. Dissociation curves were generated to ensure the specificity of each qRT-PCR reaction. The relative expression levels of validated genes in each sample (TTT_0, TTT_{14}, and TTT_{21}) were calculated and quantified using the $2^{-\Delta\Delta Ct}$ method.

Statistical analysis

All clinical data were statistically analyzed using SPSS 25.0 software (International Business Machines Corp., USA). Normally distributed data are expressed as the mean ± SD. Multiple groups with equal variances were compared by one-way analysis of variance followed by the least significant difference test; data with unequal variances were compared by Welch's approximate analysis of variance, followed by Dunnett's T3 test. For samples that did not obey a normal distribution, the measured results are expressed as the median (interquartile range) [M (P25, P75)]. When comparing the differences in the observed indicators between the two groups, the Mann–Whitney *U* test was used. When comparing the differences in observation indices between multiple groups, the Kruskal–Wallis *H* rank sum test was selected, and the Bonferroni–Holm method was used to counteract the problem of multiple comparisons. The DEPs and immune response indicators at key time points after TTT surgery were measured using R, version 4.0.3 (The R Foundation for Statistical Computing). A *P* value <0.05 indicated that the difference was statistically significant.

Study approval

This study was approved by the ethics committee following the Declaration of Helsinki (project no. S20240201-01). Informed consent was obtained from all individual participants included in the study. Data supporting the findings of this study are derived from the corresponding author upon request. Finally, sex was a biological variable, but it was unknown whether the findings were relevant for female patients.

Results

Tibial cortex transverse transport surgery can effectively promote wound healing with a high limb salvage rate

The design and workflow of the study focus on the specific clinical efficacy and the mechanism of TTT surgery (Fig. 1). Finally, a cohort of 68 patients with severe type 2 DFUs (Wagner grade III/IV) underwent TTT surgery in our cross-sectional and experimental study, and the detailed patient descriptions are shown in Table 1. The locations of DFUs were statistically analyzed, including bilateral DFUs (7.4%), unilateral DFUs (92.6%), right foot (52.9%), and left foot (39.7%). A total of 13 patients (11 males and two females) had amputation (7.4%) and death (11.8%). The statistical results showed that the DFUs of patients were well controlled, and the limb salvage rate of this technique was 92.6% (63/68). More importantly, the ideal effects were observed in patients with unilateral or bilateral DFUs, even when TTT surgery was carried out on only one side with a higher Wagner score (Fig. 2B, C, and D). Five patients with bilateral DFUs were all cured without death or amputation (7.4%). Notably, 64.7% (44/68) of patients did not use antibiotics during the entire TTT surgery, but the infections were well controlled, and the wounds healed well. As observations in clinical, wound infection can be effectively controlled, and ulcer recurrence can be significantly reduced for patients with a large amount of scar tissue. The main complications of TTT surgery in patients with DFUs include nail tract (4.4%) and incision infection (2.9%). Moreover, postprandial

Table 1

Clinical parameters of patients in the severe type 2 diabetic foot ulceration cohort treated with tibial cortex transverse transport surgery.

Clinical parameters	Male (*n* = 49)	Female (*n* = 19)	*t*/*Z*	*P*
Age (years old)	63 ± 12	68 ± 14	1.514	0.135
Diabetes history (years)	10 ± 7	11 ± 10	0.436	0.664
Time for wound healing (days)*	80 ± 36	65 ± 23	-1.610	0.113
DED	32	13	0.059	0.809
Cardiovascular disease	24	10	0.072	0.789
Usage of antibiotics	17	7	0.027	0.869
Well-controlled glucose	13	5	0.001	0.986
Location of DFUs			0.000	1.000
Bilateral DFUs	4	1	–	–
Unilateral DFUs	45	18	–	–
Right foot	28	8	–	–
Left foot	17	10	–	–
Wagner classification			0.202	0.654
III	28	12	–	–
IV	21	7	–	–
DKD			3.108	0.683
I	3	0	–	–
II	5	2	–	–
III	19	6	–	–
IV	8	5	–	–
V	2	0	–	–
Non-DKD	12	6		
Postoperative outcome			3.160	0.532
Infected nail tract	3	0	–	–
Infected incision	1	1	–	–
Amputation	4	1	–	–
Death	7	1	–	–
None	34	16	–	–

*11 male patients and two females patients had missing data due to amputation and death.
DED, diabetic eye disease; DFU, diabetic foot ulceration; DKD, diabetic kidney disease.

glucose, fasting glucose, the glomerular filtration rate, hemoglobin A1c, hemoglobin, total protein, and the ankle–brachial index were also statistically analyzed (Supplementary Table 1, Supplemental Digital Content 1, http://links.lww.com/JS9/C941). Glucose metabolism and kidney function are the major metabolic problems in patients with DFUs. Compared with those before TTT surgery, postprandial glucose, fasting glucose, glomerular filtration rate, and hemoglobin A1c were lower ($P < 0.05$).

Upward transport started to activate the systemic immune response, and wound healing occurs with downward transport during tibial cortex transverse transport surgery in patients with severe diabetic foot ulcerations

To verify our hypothesis that TTT surgery activates the immune system, engaging it in the fight against infection and thus promoting wound healing, our study was carefully designed, and flow diagrams of systematic proteomics analysis, spatially resolved metabolomics analysis, clinical immune biomarker analysis, and transcriptomics analysis for this study are shown in Figure. 1. According to the standard operation procedures, 68 patients with unilateral or bilateral DFUs underwent TTT surgery. Serum samples from patients at six-time points ($N = 30$, TTT_0, TTT_3, TTT_7, TTT_{14}, TTT_{21}, and TTT_{35}) were subjected to proteomic analysis, and the results were highly accurate and stable (Supplementary Fig. 1, Supplemental Digital Content 1, http://links.lww.com/JS9/C941). A total of 252 DEPs were identified ($P < 0.05$ and FC > 1.2). An unsupervised clustering method was used to perform cluster analysis on protein abundance values with statistically significant differences between sample groups, and ten changing trends were identified (Supplementary Fig. 2, Supplemental Digital Content 1, http://links.lww.com/JS9/C941).

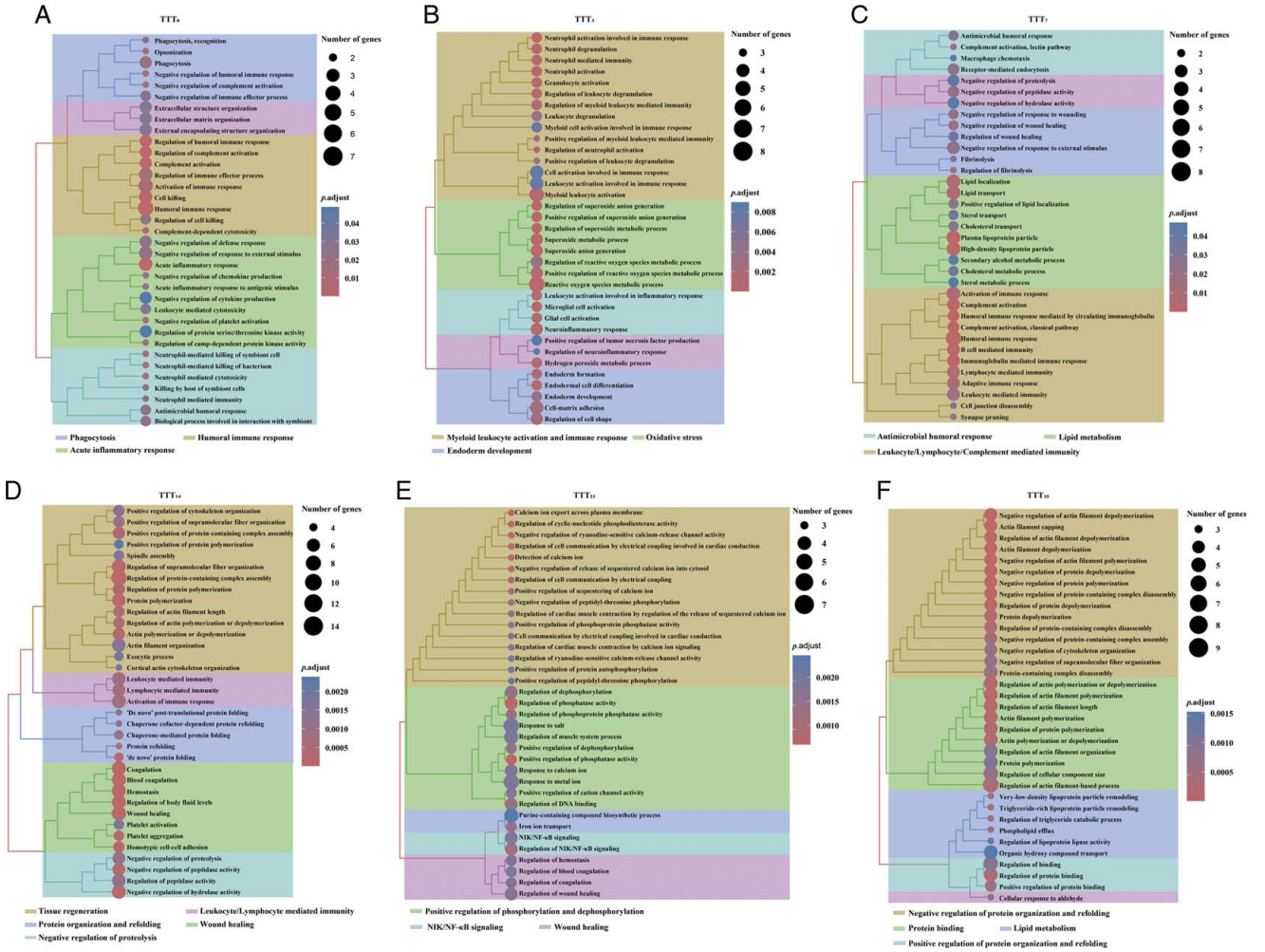

Figure 3. Terms of biological process in pathway enrichment analyses for DEPs from patients with DFUs treated with TTT surgery. A total of 252 DEPs were identified. Next, the Mfuzz package was used to analyze protein expression trends during surgery, and pathway enrichment analyses were subsequently performed on the GO database at each time point based on the temporal trend of protein expression. The BP terms used for pathway enrichment analyses are shown. The main biological processes associated with the DEPs at TTT_0 (A) were acute inflammatory response, humoral immune response, and phagocytosis; at TTT_3 (B), were myeloid leukocyte activation and immune response, oxidative stress, and endoderm development; at TTT_7 (C) were antimicrobial humoral response, lipid metabolism, and leukocyte/lymphocyte/complement-mediated immunity; at TTT_{14} (D) were tissue regeneration, leukocyte/lymphocyte-mediated immunity, protein organization and refolding, wound healing, and negative regulation of proteolysis; at TTT_{21} (E) were positive regulation of phosphorylation and dephosphorylation, NIK/NF-κB signaling, and wound healing; and at TTT_{35} (F) were positive/negative regulation of protein organization and refolding, protein binding, and lipid metabolism. DEP, differentially expressed protein; DFU, diabetic foot ulceration; TTT, tibial cortex transverse transport.

Next, we used the Mfuzz package to analyze the time trend of protein expression, and six clusters along the time points of TTT surgery were identified (Supplementary Fig. 3, Supplemental Digital Content 1, http://links.lww.com/JS9/C941). Pathway enrichment analyses of biological processes are shown in Figure 3. At the TTT_0 phase, patients with DFU were in an acute inflammatory state in which humoral immune-mediated phagocytosis was the primary immune response (Fig. 3A). At TTT_3, myeloid leukocytes (neutrophils) were consistently active, and the overall regulation of both immune and oxidative stress levels was increased in patients with DFUs. Myeloid endoderm-mediated tissue regeneration was identified for the first time (Fig. 3B). At TTT_7, patients with DFUs exhibited an antibacterial infection response as well as upregulated lipid metabolism. Moreover, the immune system, such as humoral immunity, B cells, and the complement system, was further mobilized (Fig. 3C). At TTT_{14}, the immune system of patients with DFUs underwent dynamic homeostatic regulation. In positive regulation, immune responses are sustained and mediated by leukocytes and lymphocytes. The organization of proteins and the assembly of protein complexes are upregulated to promote wound healing (Fig. 3D). At TTT_{21}, protein function (dephosphorylation, phosphoprotein phosphatase activity, and ion mobilization) and DNA biosynthesis were further upregulated for wound healing (Fig. 3E). At TTT_{35}, lipoprotein synthesis, assembly, and protein functionalization, which are required for tissue repair, continued to increase, but negative regulation of protein organization and refolding and protein binding occurred (Fig. 3F). Our results validated that the systemic immune response begins with upward transport, and wound healing occurs with downward transport during TTT surgery in patients with severe DFUs. Totally, TTT surgery activates a systemic immune response against infection to promote wound healing in patients with severe type 2 DFUs.

The crucial management strategies for TTT technology include upward transport (7 mm, 1 mm/day) and downward transport (7 mm, 1 mm/day). Compared with those in TTT_0, upregulated proteins (FC $>$ 1.5 and $P < 0.05$) and downregulated proteins (FC $<$ 0.3 and $P < 0.05$) in the stages of upward transport (at TTT_{14}), downward transport (at TTT_{21}) and the entire treatment process (at TTT_{35}) were validated through comparative analysis of volcano plots (Fig. 4A-D), protein–protein interactions (Fig. 4E–H), and Venn diagrams (Fig. 4I and G). Five proteins (P24592, P62263, Q02878, Q9H4B7, and P23634) were commonly upregulated during the upward and downward migration processes, while P02786, P50991, P62987, Q969T9, and Q9H7Z3 increased only in the upward transport. P53680, P05198, and Q99798 were upregulated only during downward migration. The only protein that was downregulated during upward migration was P26022. The serum levels of Q53RD9, P12318, and P42574 were lower after TTT surgery than before TTT surgery (Table 2).

Tibial cortex transverse transport surgery downregulated the levels of stearoylcarnitine and the glycerophospholipid metabolism pathway in skin tissue from patients with severe diabetic foot ulcerations

Since TTT surgery effectively promoted the infection resistance and tissue repair of patients with DFUs by enhancing the immune response, spatially resolved metabolomics analysis was performed to characterize immunity-related metabolites and their spatial distribution in the skin tissues of patients with DFUs at three time points: TTT_0, TTT_{14}, and TTT_{21}. Crucial processing of skin tissue samples for spatial metabolomics analysis included metabolite spatial distribution (Fig. 5A), OPLS-DA of spatial metabolomics datasets (Fig. 5B and C), and representative mass spectra of DFU skin tissues (Fig. 5D-F). Finally, a total of eight differentially abundant metabolites were identified, namely, L-palmitoylcarnitine, stearoylcarnitine, canthaxanthin A, elemonic acid, levocarnitine propionate, theobromine, triacetin and camelliagenin. Compared with those in TTT_0, the relative levels of canthaxanthin A, levocarnitine propionate, theobromine, and triacetin in the tissue were upregulated, while L-palmitoylcarnitine and stearoylcarnitine were downregulated in TTT_{14}. Compared with those in TTT_0, the relative levels of canthaxanthin were upregulated, and stearoylcarnitine and elemonic acid were downregulated in TTT_{21}. The relative content of the most common metabolite, stearoylcarnitine, decreased at TTT_{14} and TTT_{21} compared with TTT_0 (Fig. 5G-I). KEGG pathway enrichment was applied to analyze the differentially abundant metabolites from DFU tissues at TTT_0, TTT_{14}, and TTT_{21}, and carnitine metabolism was the main metabolic pathway (Fig. 5J-L). The spatial distributions of eight differentially abundant metabolites in skin tissue with DFUs are shown in Figure 6. As the skin tissue of diabetic feet was more necrotic, overall metabolism was low, and only a few metabolites were validated. However, our pathological results also revealed that the cavities in the skin tissue decreased over time, which provided direct clinical evidence that the TTT technique facilitated the repair of foot ulcers in patients (Fig. 5 A).

The specific immunomodulatory biomarkers were verified to change with the stage of tibial cortex transverse transport surgery in patients with severe type 2 diabetic foot ulcerations

Immune biomarker analysis was used to validate the specific alterations in immune molecules. Therefore, the levels of leukocytes and their subtypes, lymphocytes and their subpopulations, 12 cytokines, several immunoglobulins, and two types of complement proteins (C3 and C4) in blood from patients with DFUs treated with TTT surgery at six-time points were statistically analyzed. Due to amputation, death, and lost follow-up, the number of patients enrolled in clinical immune biomarker analysis was not the same. The Mfuzz package was also used to analyze the changes in the expression of immune response biomarkers, and six clusters were validated over time after TTT surgery (Supplementary Fig. 4, Supplemental Digital Content 1, http://links.lww.com/JS9/C941). Statistical analysis of immune indicators in each period revealed that the immune system was dominated by humoral immunity (IgG and NK cells) at TTT_0. At TTT_3, helper T lymphocytes ($CD3^+CD4^+$) and B lymphocytes ($CD19^+$) were activated, and the number of neutrophils increased. At TTT_7, the number of granulocytes, such as neutrophils and monocytes, increased rapidly, and the levels of the cytokines IL-6 and IL-17 also increased significantly. At TTT_{14}, complement proteins and IFN-α were involved in the main immune response. At TTT_{21}, $CD3^+CD8^+$ T lymphocytes and eosinophils became the dominant immune responder molecules. At TTT_{35}, the activity of the immune system in patients with DFUs was significantly better than that before surgery, represented by $CD3^+CD8^+$ T lymphocytes, $CD16^+CD56^+$ cells (NK

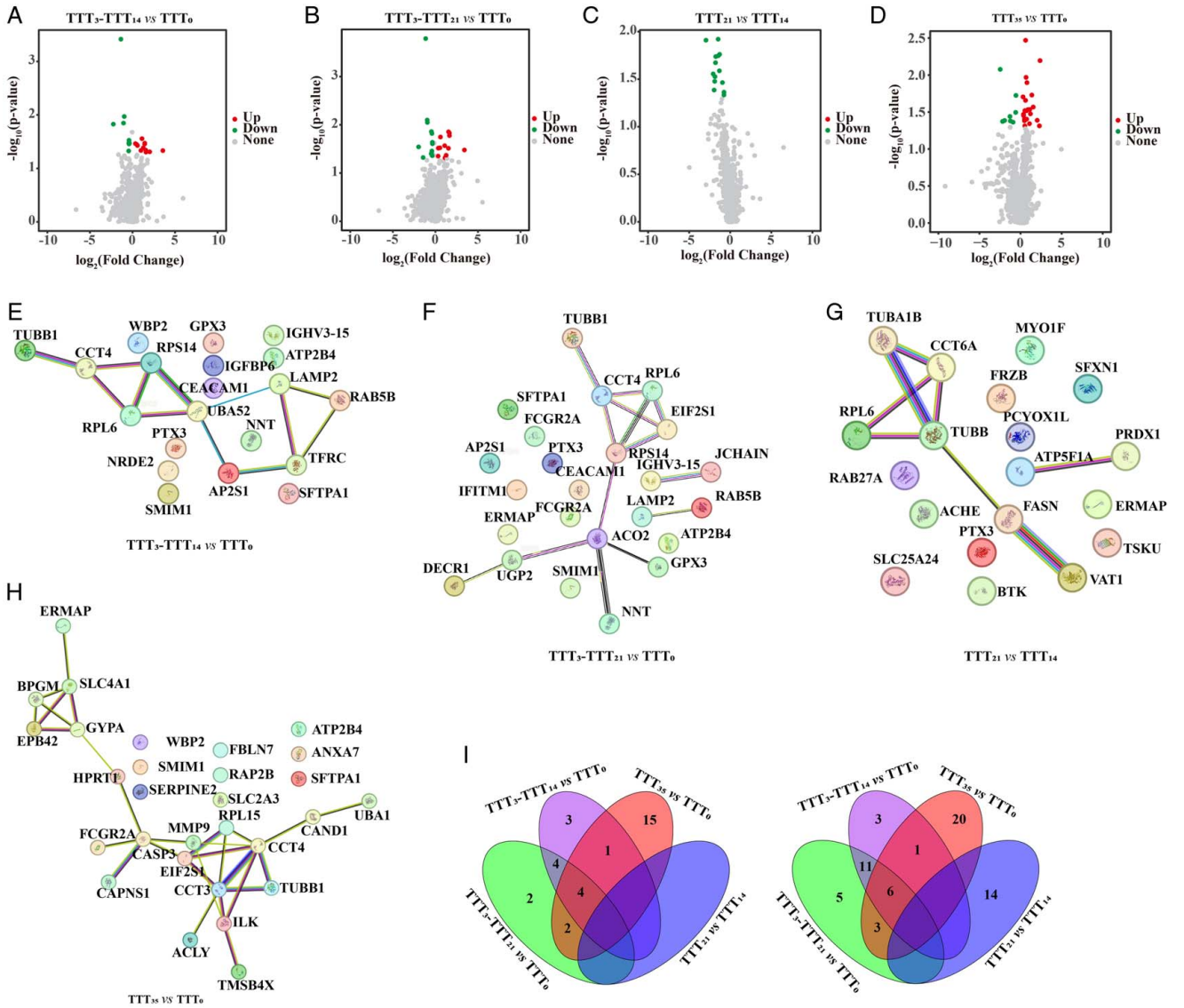

Figure 4. DEPs in TTT_{14}, TTT_{21}, and TTT_{35} compared with TTT_0. (A–D) Volcano plot showing the DEPs. Each point represents a regulated protein and the position along the x-axis represents the fold change in abundance. The thresholds for upregulated differential proteins were FC > 1.2 and *P* value < 0.05 and FC < 0.3 and *P* value < 0.05 for downregulated differential proteins. Green dots, red dots, and gray dots represent significantly upregulated, downregulated, and unchanged proteins, respectively. (H) The PPI network analysis of DEPs from the TTT_{14}, TTT_{21}, and TTT_{35} stages compared with TTT_0. (G and I) Comparative analysis of Venn diagrams for TTT_{14}, TTT_{21}, and TTT_{35} compared with TTT_0. DEP, differentially expressed protein; TTT, tibial cortex transverse transport.

cells), kappa light chain, lambda light chain, eosinophils, IgG and IL-17 (Table 3). The above results further confirmed that TTT surgery can activate the immune response in patients with DFUs.

Differential genes and enrichment signal pathways regulated wound healing and immune response in skin tissue from patients with severe diabetic foot ulcerations by tibial cortex transverse transport surgery

HE results from spatially resolved metabolomics analysis showed the cavities in the skin tissue decreased over time. For further study of the regulated genes and enrichment signal pathways in wound healing and immune response, transcriptomics was applied to analyze the skin tissue from patients with severe DFUs ($N = 3$, TTT_0, TTT_{14}, and TTT_{21}). The score plot of the PCA model was used for the first three principal component analyses of the data of TTT_0, TTT_{14}, and TTT_{21} groups (Fig. 7A). A total of 7988 genes were identified and subjected to statistical analysis. A total of 994 up and downregulated genes were identified based on FPKM $\geq$ 0.5 and *P* value < 0.05, which showed by volcano plot for TTT_{14} versus TTT_{14} (Fig. 7B), TTT_{21} versus TTT_0 (Fig. 7C), and TTT_{21} versus TTT_{14} (Fig. 7D). Pathway analysis by mapping genes to the KEGG pathway and the enrichment score value of the pathway ID was arranged in order. The top eight pathways were drawn in Figure 7E-G. As shown, the upregulated signal pathways by KEGG analysis were mainly in extracellular matrix (ECM)-receptor interaction, Fc gamma R-mediated phagocytosis, and metabolic pathways, including glycerophospholipid metabolism, while the downregulated

Table 2

The key regulated proteins in the stages of upward transport, downward transport, and the entire treatment process induced by tibial cortex transverse transport surgery in patients with diabetic foot ulcerations compared with tibial cortex transverse transport$_0$ patients.

Stage	Accession	Protein names	Gene names	FC	*P* value	KEGG	Gene ID
TTT_3-TTT_{21} vs. TTT_0 And TTT_3-TTT_{14} vs. TTT_0	P24592	Insulin-like growth factor-binding protein-6	IGFBP-6	10.61	0.03	hsa:3489	3489
	P62263	Small ribosomal subunit protein uS11	RPS14	3.14	0.02	hsa:6208	6208
	Q02878	Large ribosomal subunit protein eL6	RPL6	2.91	0.01	hsa:6128	6128
	Q9H4B7	Tubulin beta-1 chain	TUBB1	1.51	0.02	hsa:81027	81027
	P23634	Plasma membrane calcium-transporting ATPase 4	ATP2B4	1.25	0.04	hsa:493	493
TTT_3-TTT_{14} vs. TTT_0	P02786	Transferrin receptor protein 1	TFRC	1.99	0.05	hsa:7037	7037
	P50991	T-complex protein 1 subunit delta	CCT4	2.99	0.05	hsa:10575	10575
	P62987	Ubiquitin-ribosomal protein eL40 fusion protein	UBA52	2.69	0.03	hsa:7311	7311
	Q969T9	WW domain-binding protein 2	WBP2	2.40	0.04	hsa:23558	23558
	Q9H7Z3	Nuclear exosome regulator NRDE2	NRDE2	4.06	0.05	hsa:55051	55051
TTT_3-TTT_{21} vs. TTT_0	P53680	AP-2 complex subunit sigma	AP2S1	2.13	0.03	hsa:1175	1175
	P05198	Eukaryotic translation initiation factor 2 subunit 1	EIF2S1	2.18	0.05	hsa:1965	1965
	Q99798	Aconitate hydratase	ACO2	2.40	0.04	hsa:50	50
TTT_{35} vs. TTT_0	Q96PL5	Erythroid membrane-associated protein	ERMAP	5.17	0.01	hsa:114625	114625
	P50991	T-complex protein 1 subunit delta	CCT4	4.91	0.05	hsa:10575	10575
	P07738	Bisphosphoglycerate mutase	BPGM	4.08	0.04	hsa:669	669
	Q969T9	WW domain-binding protein 2	WBP2	2.91	0.03	hsa:23558	23558
	P05198	Eukaryotic translation initiation factor 2 subunit 1	EIF2S1	2.59	0.02	hsa:1965	1965
	P02724	Glycophorin-A	GYPA	2.30	0.03	hsa:2993	2993
	P00492	Hypoxanthine-guanine phosphoribosyltransferase	HPRT1	2.17	0.03	hsa:3251	3251
	P22314	Ubiquitin-like modifier-activating enzyme 1	UBA1	2.13	0.05	hsa:7317	7317
	P53396	ATP-citrate synthase	ACLY	1.85	0.03	hsa:47	47
	P02730	Band 3 anion transport protein	SLC4A1	1.71	0.01	hsa:6521	6521
	P16452	Protein 4.2	EPB42	1.68	0.04	hsa:2038	2038
	Q9H4B7	Tubulin beta-1 chain	TUBB1	1.64	0.03	hsa:81027	81027
	Q13418	Integrin-linked protein kinase	ILK	1.59	0.01	hsa:3611	3611
	P23634	Plasma membrane calcium-transporting ATPase 4	ATP2B4	1.53	0.00	hsa:493	493
	P62328	Thymosin beta-4	TMSB4X	1.52	0.02	hsa:7114	7114
TTT_3-TTT_{14} vs. TTT_0	P26022	Pentraxin-related protein PTX3	PTX3	0.21	0.01	hsa:5806	5806
TTT_{35} vs. TTT_0	Q53RD9	Fibulin-7	FBLN7	0.18	0.01	hsa:129804	129804
	P12318	Low-affinity immunoglobulin gamma Fc region receptor II-a	FCGR2A	0.22	0.04	hsa:2212	2212
	P42574	Caspase-3	CASP3	0.26	0.04	hsa:836	836

FC, fold change; upregulated proteins, FC > 1.2 and *P* value < 0.05; downregulated proteins, FC < 0.3 and *P* value < 0.05.
KEGG, Kyoto Encyclopedia of Genes and Genomes; TTT, tibial cortex transverse transport.

pathways were PPAR signaling pathway, protein processing in the endoplasmic reticulum, diabetic cardiomyopathy, and so on.

Further, 67 genes from the pathway and GO analysis based on their functions, higher values of FPKM, and *P* value < 0.05 were screened out and were quantitatively analyzed by RT-qPCR. As shown in Figure 7H, the expression of PRNP (prion protein), which regulated the immune response, was statistically significant at TTT_{14} ($P < 0.01$) and TTT_{21} ($P < 0.01$) when compared with TTT_0. The pathway analysis showed that PLCB3 (PLCB3, phospholipase C beta 3) and VE-cadherin play roles in vascular smooth muscle contraction, and the results of RT-qPCR validated that the expression of PLCB3 was statistically significant at TTT_{14} ($P < 0.05$) and TTT_{21} ($P < 0.001$) when compared with TTT_0, the differential expression of VE-cadherin was statistically significant at TTT_{21} ($P < 0.05$) when compared with TTT_0. The genes that handled the developmental process were also quantitatively analyzed, and the expression of PPDPF (pancreatic progenitor cell differentiation and proliferation factor) and LAMC2 (laminin subunit gamma 2) was statistically significant at TTT_{14} ($P < 0.001$) and TTT_{21} ($P < 0.001$) when compared with TTT_0, the differential expression of SPRR2G (small proline-rich protein 2G) was statistically significant at TTT_{21} ($P < 0.05$) when compared with TTT_0. Despite not being statistically significant, parts of other genes showed obvious trends in change were shown.

Discussion

For the first time, we provided direct clinical evidence that TTT surgery can be used to treat severe DFUs unilaterally or bilaterally in type 2 patients. A total of 13 patients (11 males and two females) had amputation (7.4%) and death (11.8%). The statistical results showed that the DFUs of patients were well controlled, and the limb salvage rate of this technique was 92.6%. Five patients with bilateral DFUs were all cured without death or amputation (7.4%). Notably, 64.7% of patients did not use antibiotics during the entire TTT surgery, but the infections were well controlled, and the wounds healed well. The main complications of TTT surgery in patients with DFUs include nail tract (4.4%) and incision infection (2.9%).

Based on our clinical data, we further hypothesize that TTT surgery may activate a systemic immune response against infection to promote wound healing in patients with severe type 2 DFUs. First, integrated proteomics, spatially resolved

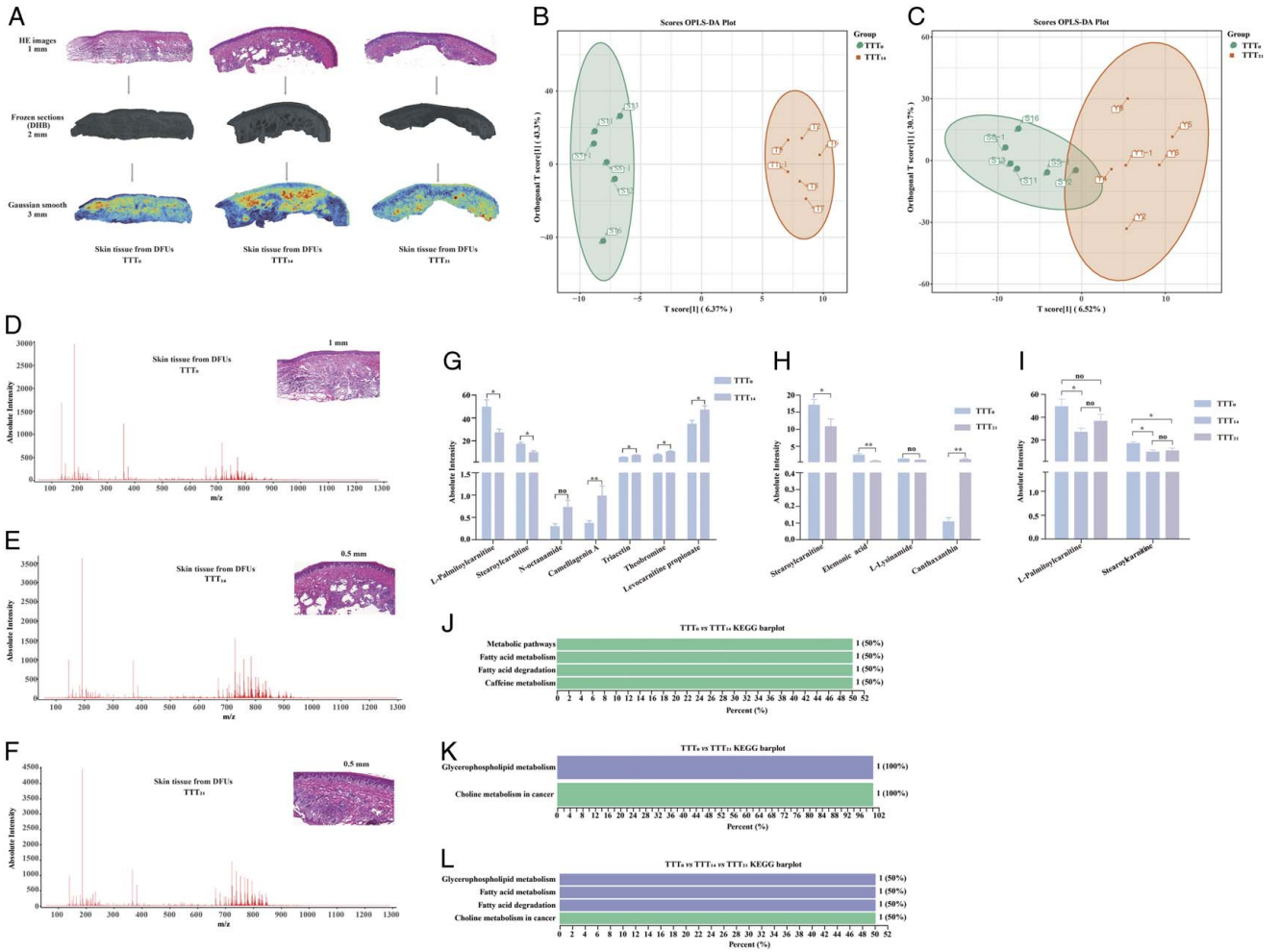

Figure 5. Spatially resolved metabolomics analysis of DFU skin tissues. (A) Crucial processing of skin tissue samples for spatial metabolomics analysis, including H&E staining of skin tissue sections, DHB matrix spraying of frozen sections, and metabolite spatial distribution with Gaussian smoothing. (B and C) OPLS-DA of spatial metabolomics datasets. (D–F) Representative mass spectra of DFU skin tissue (TTT_0, TTT_{14}, and TTT_{21}). (G–I) The bar diagram shows the expression levels of differentially abundant metabolites in glycerophospholipid, fatty acid, and glycerophospholipid metabolism pathways at TTT_{14} and TTT_{21} compared with TTT_0. A total of eight differentially abundant metabolites were identified in TTT_0, TTT_{14}, and TTT_{21}, and their change trends were statistically analyzed. (J–L) Bar plot of KEGG pathway enrichment analysis for the differentially abundant metabolites. The glycerophospholipid metabolism pathway was validated in DFU skin tissues. ***P* value <0.005; **P* value <0.05. DFU, diabetic foot ulceration; KEGG, Kyoto Encyclopedia of Genes and Genomes; TTT, tibial cortex transverse transport.

metabolomics, and clinical immune biomarker analyses were designed to verify our hypothesis. Overall, the immune response induced by TTT surgery at different time points was first comprehensively examined. In our study, we further confirmed the function of transverse transport in the upward and downward tibial cortexes. The upward transport mainly activated the systemic immune response, and the downward transport promoted wound healing. At TTT_0, the overall immune status of patients with DFUs was inactive. At TTT_3, myeloid leukocytes (mainly neutrophils) are first activated to mediate the anti-inflammatory response in patients with DFUs after TTT surgery. Next, the systemic immune response begins with upward movement (TTT_7), and wound healing occurs with upward movement (TTT_{14}). At TTT_7–TTT_{14}, systemic immune responses, including humoral immunity, B cells, IFN-α, and the complement system, were further sustained. Starting with TTT_{14}, TTT surgery mainly promoted wound healing by regulating protein synthesis, assembly, protein functionalization, and tissue regeneration. Moreover, a series of key proteins involved in immune modulation and wound healing were identified through label-free proteomic analysis. For example, the expression of IGFBP-6 (insulin-like growth factor-binding protein-6, FC = 10.61) was upregulated by TTT surgery. It has been verified to play a possible role in the immunological response and tissue repair[25,26]. ERMAP (erythroid membrane-associated protein, FC = 5) has been validated as a B7 family-related molecule that negatively regulates T-cell and macrophage responses[27]. Highly expressed CCT4 can regulate the actin cytoskeleton and impair proteostasis[28]. Similarly, TTT surgery upregulated the expression of CCT4 (FC = 4.91). In addition, the specific functions and roles of these candidate proteins need to be further verified.

Metabolic reprogramming and its metabolites are involved in the pathogenesis of immune-related inflammatory diseases, such as diabetes[29,30]. The proteomic analysis also revealed the regulation of lipid metabolism in patients with DFUs. Therefore, the spatial metabolism characteristics of skin tissue from patients

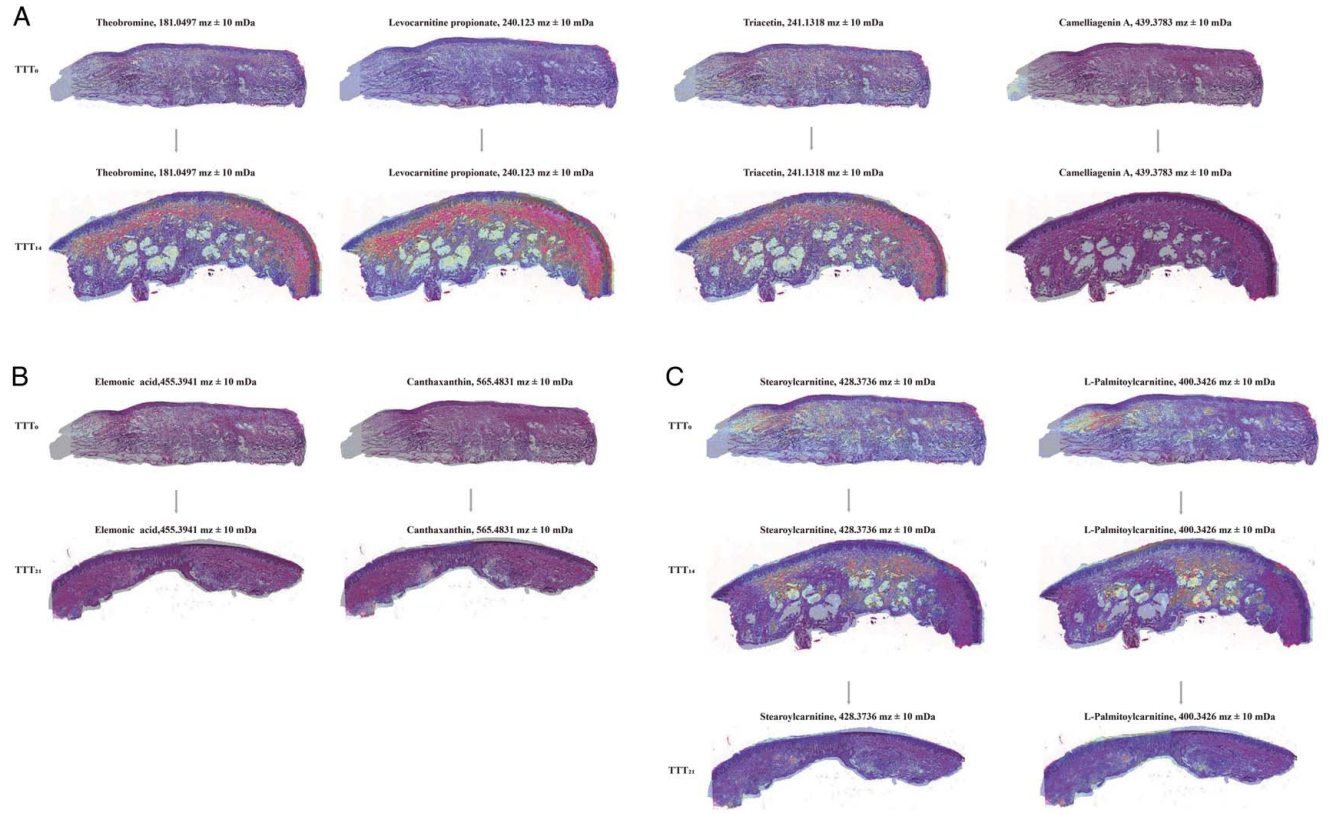

Figure 6. Spatial expression images of differentially abundant metabolites in DFU tissue sections based on spatially resolved metabolomics data (intensity in color scale is relative value). (A) Expression and spatial distributions of theobromine, levocarnitine propionate, canthaxanthin A, and triacetin at TTT_{14} compared with those at TTT_0. (B) Expression and spatial distributions of elemonic acid and camelliagenin at TTT_{21} compared with those at TTT_0. (C) Decreased concentrations of L-palmitoylcarnitine and stearoylcarnitine in DFU tissues from TTT_{14} and TTT_{21} patients compared with those of TTT_0 patients. *P value <0.05, **P value <0.01. DFU, diabetic foot ulceration; TTT, tibial cortex transverse transport.

with DFUs were described for the first time by spatially resolved metabolomics analysis in our study. Stearoylcarnitine was the most important metabolite, and its tissue levels decreased over the recovery of the wound; glycerophospholipid metabolism was the main metabolic pathway. The accumulation of carnitines is associated with the poor immune recovery and activated proinflammatory signaling pathways[31,32]. Therefore, TTT surgery may promote the recovery and enhancement of immune function by downregulating the levels of stearoylcarnitine and glycerophospholipid metabolism in the skin tissue of patients with severe DFUs.

The results of the cluster analysis of clinical immune biomarkers were consistent with the proteomic analysis and further verified that TTT surgery induced specific immunomodulation in patients with DFUs. Leukocytes (neutrophils, monocytes, and eosinophils), cytokines (IL-6, IL-17, and IFN-α), complement proteins (C3 and C4), and $CD3^+CD4^+$ T lymphocytes, which evolve into $CD3^+CD8^+$ T lymphocytes at TTT_{21}, and $CD19^+$ B lymphocytes are the dominant immune response biomarkers. Leukocytes and granulocytes may have anti-inflammatory and anti-infection effects. Neutrophils are highly abundant circulating leukocytes that are among the first cells to be recruited to sites of infection or sterile injury and may be anti-inflammatory agents that may further promote the clearance of dead cells and the reprogramming of macrophages to promote resolution and repair[33]. An increase in IL-6 may further reduce inflammation, promote T-cell proliferation, and promote host defense against extracellular bacterial and fungal infections[34,35]; IL-17 also increases immune responses against human fungal pathogens[36]. The upregulation of IFN-α in the serum of patients with DFUs may have protective effects on the promotion of T-cell, dendritic cell, monocyte, NK cell, and B-cell responses during infection with viruses, bacteria, parasites, and fungi[37]. The complement system may have a positive role in both innate and adaptive immune responses, and the consequences of these interactions on host defense against common pathogens include bacteriolysis and cell lysis, opsonized phagocytosis, immune adhesion, and so on[38,39]. $CD3^+CD4^+$ T lymphocytes and $CD19^+$ B lymphocytes can directly activate the protective immune response against infection. Importantly, a feature of a successful immune response was the production of memory $CD3^+$ $CD8^+$ T cells at TTT_{21}. This study is the first to dynamically validate and monitor the ability of TTT surgery to activate the immune system to promote wound healing in patients with DFU.

As the results of transcriptomics and RT-qPCR showed, the upregulated signal pathways were mainly in ECM-receptor interaction, Fc gamma R-mediated phagocytosis, and metabolic pathways, including glycerophospholipid metabolism. Fc gamma R-mediated phagocytosis can promote patients with DFUs to eliminate infection[40]. Tissues are dynamically shaped by bidirectional communication between resident cells and the ECM through cell–matrix interactions and ECM remodeling[41]. So,

Table 3

Clinical immunological response biomarkers in patients with diabetic foot ulcerations treated with tibial cortex transverse transport surgery.

Time point	Clinical immunological biomarkers	Mean ± SD	RI	Units
TTT_0	IgA	3.258 ± 1.352	1.00–4.20	g/l
	$CD16^+CD56^+$ cells (NK Cells) AVs	196.206 ± 170.782	150.00–900.00	pieces/μl
	Kappa light chain	3.290 ± 1.307	1.70–3.70	g/l
	Lymphocyte	0.194 ± 0.106	20.00–50.00	%
TTT_3	B lymphocytes	13.846 ± 6.709	5.00–20.00	%
	$CD19^+$ (B lymphocytes) AVs	204.600 ± 140.630	90.00–580.00	pieces/μl
	Leukocytes	10.223 ± 4.417	3.50–9.50	10^{*9}/l
	$CD4^+/CD8^+$ ratios	1.722 ± 0.794	0.71–2.78	%
	IgE	158.260 ± 281.482	< 100	IU/ml
	Neutrophil	7.986 ± 4.205	1.80–6.30	10^{*9}/l
	$CD3^+CD4^+$T lymphocytes	41.081 ± 10.172	27.00–51.00	%
	Neutrophil	0.747 ± 0.093	40.00–75.00	%
	Lymphocytes	1.412 ± 0.615	1.10–3.20	10^9/l
TTT_7	Neutrophils	0.722 ± 0.089	1.80–6.30	10^9/l
	Monocytes	0.074 ± 0.026	0.10–0.60	10^9/l
	Leukocytes	9.672 ± 6.042	3.50–9.50	10^9/l
	IL-6	102.120 ± 200.912	0.00–5.71	pg/ml
	Neutrophil	0.722 ± 0.089	40.00–75.00	%
	IL-17	12.374 ± 12.392	0.00–20.60	pg/ml
TTT_{14}	Complement C3	1.35 ± 0.253	0.70–3.70	g/l
	IFN-α	0.390 ± 0.124	0.00–8.50	pg/ml
	Complement C4	1.682 ± 1.784	0.10–0.40	g/l
TTT_{21}	Eosinophil	0.030 ± 0.020	0.40–8.00	%
	Eosinophils	0.216 ± 0.169	0.02–0.52	10^9/l
	IgG	13.933 ± 4.466	8.60–17.40	g/l
	Lambda light chain	1.951 ± 0.611	0.90–2.10	g/l
	Lymphocyte	0.191 ± 0.086	20.00–50.00	%
	$CD3^+CD8^+$ T lymphocytes	28.843 ± 8.673	15.00–44.00	%
TTT_{35}	Lymphocyte	0.191 ± 0.086	20.00–50.00	%
	$CD3^+CD8^+$ T lymphocytes	30.746 ± 9.054	15.00–44.00	%
	$CD3^+CD8^+$ T lymphocytes AVs	412.627 ± 217.633	360.00–1250.00	pieces/μl
	$CD16^+CD56^+$ cells (NK cells) AVs	166.642 ± 94.552	150.00–900.00	pieces/μl
	Kappa light chain	3.306 ± 1.086	1.70–3.70	g/l
	Lambda light chain	1.952 ± 0.613	0.90–2.10	g/l
	Lymphocyte	1.315 ± 0.477	1.10–3.20	10^9/l
	Eosinophil	0.216 ± 0.170	0.02–0.52	10^9/l
	IgG	13.933 ± 4.471	8.60–17.40	g/l
	IL-17	10.105 ± 12.004	0.00–20.60	pg/ml

AVs, absolute values; RI, reference interval; TTT, tibial cortex transverse transport.

the upregulated ECM-receptor interaction may promote wound healing in patients with DFUs. Metabolic pathways, including glycerophospholipid metabolism, are consistent with the results of spatially resolved metabolomics analysis. In the future, we will further explore genes that regulate glycerophospholipid metabolism and stearoylcarnitine to promote the recovery and enhancement of immune function in the skin tissue of patients with severe DFUs. While the PPAR signaling pathway was downregulated, TTT surgery can activate systemic cell metabolism, energy homeostasis, and immune response[42]. Besides, TTT surgery can reduce the risk of diabetic cardiomyopathy in the absence of coronary artery disease, hypertension, and significant valvular disease. First, our study validated TTT surgery may upregulate the level of PRNP to activate the immune system[43]. At the same time, TTT surgery could promote neovascularization by PLCB3[44] and VE-cadherin[44]. In this study, TTT surgery can facilitate the developmental process, mainly keratinocyte differentiation through PPDPF[45], LAMC2[46], and SPRR2G.

The current TTT surgical treatment protocol is one cycle with a total of 39 days. Prolonged hospitalization of patients is detrimental to the patient's recovery and the hospital's operation and management. In combination with our results suggesting that the TTT technique can induce an immune response, we have optimized the duration of the TTT procedure with a total of 19 days in our latest IIT study. The TTT procedure (v2.0) has achieved good outcomes (Supplementary Figure 5, Supplemental Digital Content 1, http://links.lww.com/JS9/C941). The above results indirectly proved that the key step of the TTT technique may be the upward transport, which promotes wound repair by activating the immune system. In the future, we will incorporate more patients to validate the mechanism of activating the immune system to promote wound repair by TTT surgery and promote the sustainable optimization and clinical application of TTT surgery.

Limitations

Our study has several limitations that need to be addressed. First, larger groups are needed to validate the features of the immune response induced by TTT surgery in patients with unilateral or bilateral DFUs. Second, disease complexity, individual differences, variations in surgical techniques, and postoperative management could influence outcomes and limit generalizability. As for individual differences as well as cavities in the skin tissue of DFUs, the candidate genes and metabolites showed notable trends in change but were not statistically significant. Third, the diagnostic, therapeutic, and prognostic roles of these candidate proteins and immune biomarkers for TTT surgery in patients with DFUs were not studied. Due to the inconsistency of skin repair mechanisms in mice and humans and poor mammalian surgical compliance, attempts are still being made to validate our hypothesis that the TTT technique activates the immune response to promote wound repair by establishing a true animal model of simulating patients with DFUs.

Conclusions

In summary, TTT surgery can effectively treat unilateral or bilateral type 2 severe DFU patients by inducing a systemic immune response against infection to promote wound healing. In addition, the systemic immune response begins with the upward transverse transport of the tibial cortex, and wound healing occurs with the downward transverse transport of the tibial cortex. Interestingly, stearoylcarnitine was verified as a crucial metabolite, and its spatial distribution in skin tissue from DFUs was first characterized by spatially resolved metabolomics. Firstly, candidate genes, which were induced by TTT surgery to play roles in activating the immune system, promoting neovascularization, and the developmental process, mainly

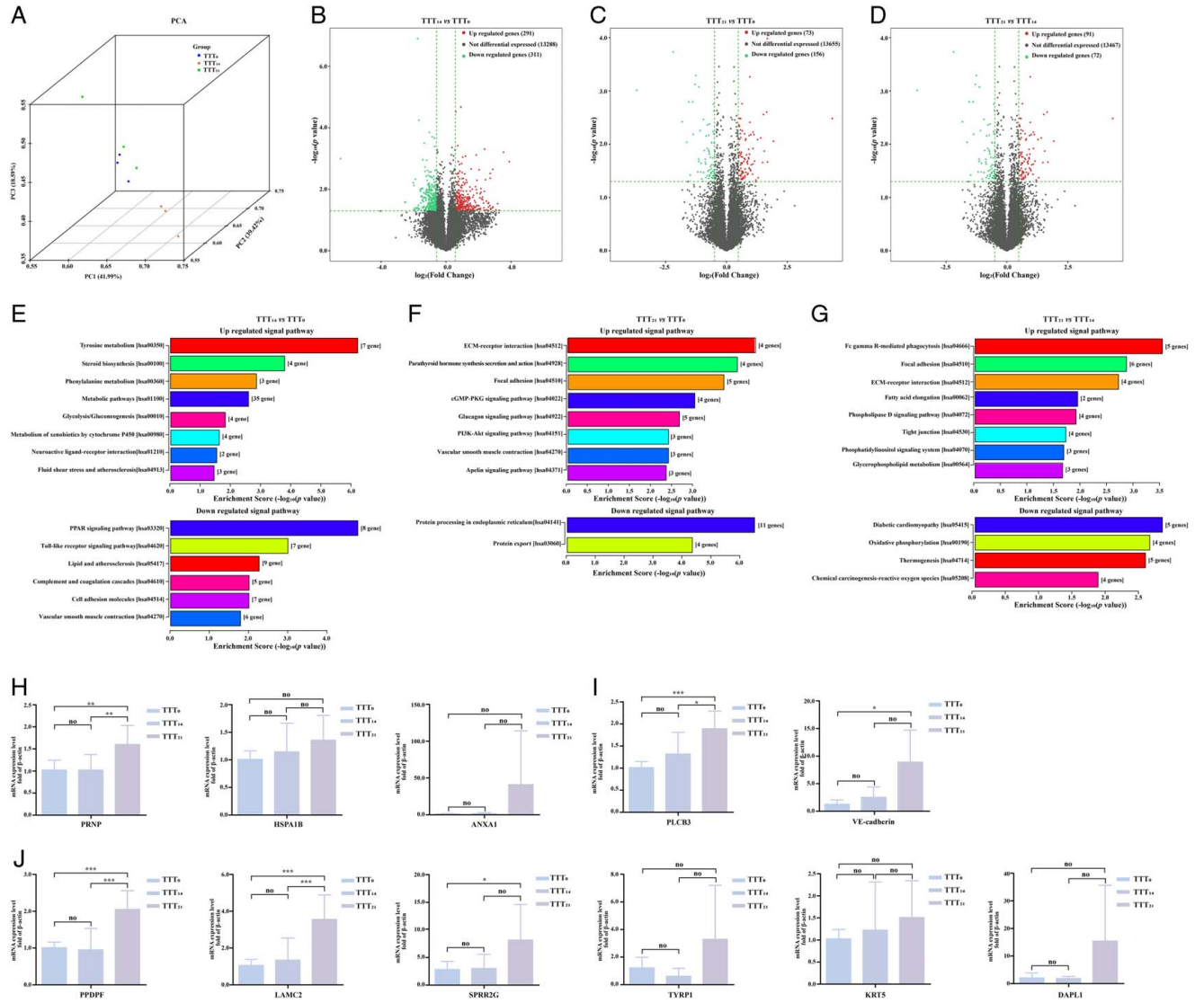

Figure 7. Differential genes and enrichment signal pathways regulated by TTT surgery. (A) Three-dimensional score plot of the PCA model of all samples. (B–D) Volcano plot showing the differential genes score plots for TTT_{14} versus TTT_{14}, TTT_{21} versus TTT_0, and TTT_{21} versus TTT_{14}. (E–G) Pathway analysis by mapping genes to the KEGG pathway for TTT_{14} versus TTT_{14}, TTT_{21} versus TTT_0, and TTT_{21} versus TTT_{14}. The expression analysis of the candidate gene regulated the immune response (H), vascular smooth muscle contraction (I), and wound healing (J) quantified by reverse-transcription quantitative PCR (RT-qPCR) in skin tissues from DFUs. Gene expression levels were normalized to the housekeeping gene (β-actin). Data were expressed as mean ± SD using the $2^{-\Delta\Delta Ct}$ method ($n = 3$ independent assays). A one-way analysis of variance analysis was carried out to evaluate statistical differences between groups (TTT_0, TTT_{14}, and TTT_{21}). *P value < 0.05; **, P value < 0.01; ***, P value < 0.001. DFU, diabetic foot ulceration; KEGG, Kyoto Encyclopedia of Genes and Genomes; TTT, tibial cortex transverse transport.

keratinocyte differentiation, were screened out and validated by transcriptomics and RT-qPCR analysis. Our research provided directions for in-depth mechanistic research on TTT surgery, and additional studies will contribute to the optimization and promotion of TTT technology in clinical practice.

Ethical approval

This study was approved by the ethics committee of Mianyang Central Hospital following the Declaration of Helsinki (project no. S20240201-01).

Consent

Informed consent was obtained from all individual participants included in the study.

Source of funding

This study was supported by Sichuan Science and Technology Program (Grant No. 2024NSFSC1522), the General Program of Natural Science Foundation of Sichuan Province (Grant No. 2022NSFSC0814), the Sichuan Province Medical (Youth Innovation) Scientific Research Project (Grant No. Q22048), the

Project of NHC Key Laboratory of Nuclear Surgery Medical Transformation (Grant No. 2022HYX014), and the Incubation Project of Mianyang Central Hospital (Grant No. 2022FH01). The analytical platform used for proteomic analysis was from Dashuo Biotech Co. Ltd (Dalian, China), the spatially resolved metabolomics platform was from MetWare Co. Ltd (Wuhan, China), and the transcriptomics platform was from Kangxiang Biotechnology Co. Ltd (Shanghai, China).

Author contributions

Lin Yu and Dingwei Zhang: conceptualization; Lin Yu, Dingwei Zhang, and Yuan Yin: methodology; Lin Yu and Yuan Yin: software; Lin Yu: validation; Lin Yu: writing – original draft preparation; Lin Yu: writing – review and editing; Dingwei Zhang, Xiaoya Li, Chunxia Bai, Daofei Xu, Xianjun Yu, and Sichun Zhao: TTT surgery treatment for patients with DFUs; Rong Hu, Xiaoya Li, Fudie Guo, and Chunxia Bai: clinical care of patients with DFUs; Qian Zhou, Xinyi Liu, Xiaoya Li, and Chunxia Bai: collection of clinical data; Qian Zhou, Xinyi Liu, Xiaojun Tian, Yan Ren, and Gang Chen: clinical laboratory tests; Yuan Yin and Yuwei Yang: clustering and statistical analysis; Jiawei Zeng, Jiafu Feng, and Dingwei Zhang: project administration; and Lin Yu and Jiawei Zeng: funding acquisition.

Conflicts of interest disclosure

The authors declare that the research was conducted in the absence of any commercial or financial relationships that could be construed as a potential conflict of interest and were grateful to patients and families for the interest and generous participation in our research effort.

Research registration unique identifying number (UIN)

Research Registry (ID # 10285).

Guarantor

Lin Yu and Dingwei Zhang.

Data availability statement

Derived data supporting the findings of this study were available from the corresponding author on request.

Provenance and peer review

Not commissioned, externally peer-reviewed.

References

[1] Harding JL, Pavkov ME, Magliano DJ, *et al*. Global trends in diabetes complications: a review of current evidence. Diabetologia 2019;62:3–16.
[2] Ceriello A, Prattichizzo F, Phillip M, *et al*. Glycaemic management in diabetes: old and new approaches. Lancet Diabetes Endocrinol 2022;10:75–84.
[3] Whittemore R, Vilar-Compte M, De La Cerda S, *et al*. Challenges to diabetes self-management for adults with type 2 diabetes in low-resource settings in Mexico City: a qualitative descriptive study. Int J Equity Health 2019;18:133.
[4] Williams R, Karuranga S, Malanda B, *et al*. Global and regional estimates and projections of diabetes-related health expenditure: Results from the International Diabetes Federation Diabetes Atlas, 9th edition. Diabetes Res Clin Pract 2020;162:108072.
[5] Armstrong DG, Tan TW, Boulton AJM, *et al*. Diabetic Foot Ulcers: A Review. JAMA. 2023;330:62–75.
[6] Ahmad E, Lim S, Lamptey R, *et al*. Type 2 diabetes. Lancet 2022;400:1803–20.
[7] Chen Y, Ding X, Zhu Y, *et al*. Effect of tibial cortex transverse transport in patients with recalcitrant diabetic foot ulcers: A prospective multicenter cohort study. J Orthop Translat 2022;36:194–204.
[8] Hua Q, Zhang Y, Wan C, *et al*. Chinese Association of Orthopaedic Surgeons (CAOS) clinical guideline for the treatment of diabetic foot ulcers using tibial cortex transverse transport technique (version 2020). J Orthop Transl 2020;25:11–6.
[9] Chen Y, Kuang X, Zhou J, *et al*. Proximal tibial cortex transverse distraction facilitating healing and limb salvage in severe and recalcitrant diabetic foot ulcers. Clin Orthop Relat Res 2020;478:836–51.
[10] Ganeshan K, Chawla A. Metabolic regulation of immune responses. Annu Rev Immunol 2014;32:609–34.
[11] Makowski L, Chaib M, Rathmell JC. Immunometabolism: From basic mechanisms to translation. Immunol Rev 2020;295:5–14.
[12] Diskin C, Ryan TAJ, O'Neill LAJ. Modification of proteins by metabolites in immunity. Immunity 2021;54:19–31.
[13] Babu M, Snyder M. Multi-omics profiling for health. Mol Cell Proteomics 2023;22:100561.
[14] Chen ZZ, Gerszten RE. Metabolomics and proteomics in type 2 diabetes. Circ Res 2020;126:1613–27.
[15] Karczewski KJ, Snyder MP. Integrative omics for health and disease. Nat Rev Genet 2018;19:299–310.
[16] Qie J, Liu Y, Wang Y, *et al*. Integrated proteomic and transcriptomic landscape of macrophages in mouse tissues. Nat Commun 2022;13:7389.
[17] Oyibo SO, Jude EB, Tarawneh I, *et al*. A comparison of two diabetic foot ulcer classification systems: the Wagner and the University of Texas wound classification systems. Diabetes Care 2001;24:84–8.
[18] Mathew G, Agha R, Albrecht J, *et al*. STROCSS 2021: strengthening the reporting of cohort, cross-sectional and case-control studies in surgery. Ann Med Surg 2021;72:103026.
[19] Alexandrov T. Spatial metabolomics and imaging mass spectrometry in the age of artificial intelligence. Annu Rev Biomed Data Sci 2020;3:61–87.
[20] Wozniak JM, Mills RH, Olson J, *et al*. Mortality risk profiling of staphylococcus aureus bacteremia by multi-omic serum analysis reveals early predictive and pathogenic signatures. Cell 2020;182:1311–27.e14.
[21] Johnson ECB, Dammer EB, Duong DM, *et al*. Large-scale proteomic analysis of Alzheimer's disease brain and cerebrospinal fluid reveals early changes in energy metabolism associated with microglia and astrocyte activation. Nat Med 2020;26:769–80.
[22] Sun C, Wang A, Zhou Y, *et al*. Spatially resolved multi-omics highlights cell-specific metabolic remodeling and interactions in gastric cancer. Nat Commun 2023;14:2692.
[23] Botling J, Micke P. Fresh frozen tissue: RNA extraction and quality control. Methods Mol Biol 2011;675:405–13.
[24] Ye S, Chen W, Ou C, *et al*. RNA sequencing reveals novel LncRNA/mRNAs co-expression network associated with puerarin-mediated inhibition of cardiac hypertrophy in mice. PeerJ 2022;10:e13144.
[25] Liso A, Venuto S, Coda ARD, *et al*. IGFBP-6: At the Crossroads of Immunity, Tissue Repair and Fibrosis. Int J Mol Sci 2022;23:4358.
[26] Venuto S, Coda ARD, González-Pérez R, *et al*. IGFBP-6 network in chronic inflammatory airway diseases and lung tumor progression. Int J Mol Sci 2023;24:4804.
[27] Su M, Lin Y, Cui C, *et al*. ERMAP is a B7 family-related molecule that negatively regulates T cell and macrophage responses. Cell Mol Immunol 2021;18:1920–33.
[28] Wang G, Zhang M, Meng P, *et al*. Anticarin-β shows a promising anti-osteosarcoma effect by specifically inhibiting CCT4 to impair proteostasis. Acta Pharma Sinica B 2022;12:2268–79.
[29] Yang W, Cong Y. Gut microbiota-derived metabolites in the regulation of host immune responses and immune-related inflammatory diseases. Cell Mol Immunol 2021;18:866–77.

[30] Zasłona Z, O'Neill LAJ. Cytokine-like roles for metabolites in immunity. Mol Cell 2020;78:814–23.
[31] Rutkowsky JM, Knotts TA, Ono-Moore KD, *et al*. Acylcarnitines activate proinflammatory signaling pathways. Am J Physiol Endocrinol Metab 2014;306:E1378–87.
[32] Chen C, Hou G, Zeng C, *et al*. Metabolomic profiling reveals amino acid and carnitine alterations as metabolic signatures in psoriasis. Theranostics 2021;11:754–67.
[33] Loh W, Vermeren S. Anti-inflammatory neutrophil functions in the resolution of inflammation and tissue repair. Cells 2022;11:4076.
[34] Rose-John S, Jenkins BJ, Garbers C, *et al*. Targeting IL-6 trans-signalling: past, present and future prospects. Nat Rev Immunol 2023;23:666–81.
[35] Weber R, Groth C, Lasser S, *et al*. IL-6 as a major regulator of MDSC activity and possible target for cancer immunotherapy. Cell Immunol 2021;359:104254.
[36] Lionakis MS, Drummond RA, Hohl TM. Immune responses to human fungal pathogens and therapeutic prospects. Nat Rev Immunol 2023;23:433–52.
[37] McNab F, Mayer-Barber K, Sher A, *et al*. Type I interferons in infectious disease. Nature Reviews Immunology 2015;15:87–103.
[38] Dunkelberger JR, Song W-C. Complement and its role in innate and adaptive immune responses. Cell Res 2010;20:34–50.
[39] West EE, Kolev M, Kemper C. Complement and the regulation of T cell responses. Ann Rev Immunol 2018;36:309–38.
[40] Fitzer-Attas CJ, Lowry M, Crowley MT, *et al*. Fcgamma receptor-mediated phagocytosis in macrophages lacking the Src family tyrosine kinases Hck, Fgr, and Lyn. J Exp Med 2000;191:669–82.
[41] Winkler J, Abisoye-Ogunniyan A, Metcalf KJ, *et al*. Concepts of extracellular matrix remodelling in tumour progression and metastasis. Nat Commun 2020;11:5120.
[42] Ahmadian M, Suh JM, Hah N, *et al*. PPARγ signaling and metabolism: the good, the bad and the future. Nat Med 2013;19:557–66.
[43] Cha S, Kim MY. The role of cellular prion protein in immune system. BMB Rep 2023;56:645–50.
[44] Bobryshev YV, Cherian SM, Inder SJ, *et al*. Neovascular expression of VE-cadherin in human atherosclerotic arteries and its relation to intimal inflammation. Cardiovasc Res 1999;43:1003–17.
[45] Ni QZ, Zhu B, Ji Y, *et al*. PPDPF promotes the development of mutant KRAS-driven pancreatic ductal adenocarcinoma by regulating the GEF activity of SOS1. Adv Sci (Weinh) 2023;10: e2202448.
[46] Colognato H, Yurchenco PD. Form and function: the laminin family of heterotrimers. Dev Dyn 2000;218:213–34.